

Progress Toward a Video-Rate, Passive Millimeter-Wave Imager for Brownout Mitigation

Daniel G. Mackrides^a, Christopher A. Schuetz^a, Richard D. Martin^a, Thomas E. Dillon^a, Peng Yao^a, and Dennis W. Prather^b

^aPhase Sensitive Innovations Inc., 51 East Main Street, Suite 201, Newark, DE 19711 USA

^bDepartment of Electrical and Computer Engineering, University of Delaware, 140 Evans Hall Newark, DE 19716 USA

ABSTRACT

Currently, brownout is the single largest contributor to military rotary-wing losses. Millimeter-wave radiation penetrates these dust clouds effectively, thus millimeter-wave imaging could provide pilots with valuable situational awareness during hover, takeoff, and landing operations. Herein, we detail efforts towards a passive, video-rate imager for use as a brownout mitigation tool. The imager presented herein uses a distributed-aperture, optically-upconverted architecture that provides real-time, video-rate imagery with minimal size and weight. Specifically, we detail phenomenology measurements in brownout environments, show developments in enabling component technologies, and present results from a 30-element aperiodic array imager that has recently been fabricated.

Keywords: upconverted passive millimeter wave imaging, brownout mitigation, distributed aperture imaging

1. INTRODUCTION

Millimeter-wave radiation lies in the electromagnetic spectrum between microwave and terahertz frequencies. All physical objects emit thermal radiation according to the Rayleigh-Jeans law. However, terrestrial objects near room temperature emit roughly eight orders of magnitude lower irradiance in the mmW spectrum as compared to the infrared spectrum. This necessitates very sensitive receivers for imaging in this regime with associated technological challenges to make mmW imaging feasible. On the other hand, there is considerable interest in using this region of the spectrum due to the fact that mmW radiation can penetrate thin dielectric materials as well as atmospheric obscurants [1]. As a result, potential applications include stand-off threat detection, portal screening, aerial reconnaissance, persistent surveillance, and situational awareness in degraded visual environments [2-6].

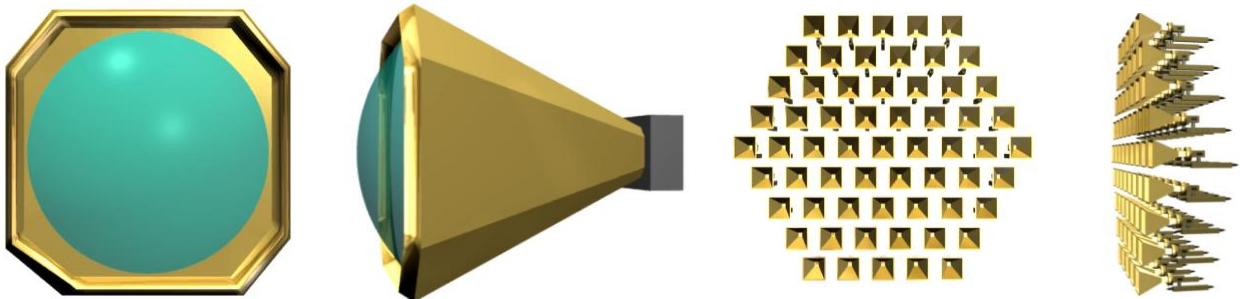


Figure 1: Three-dimensional form factor for a conventional imager relying on refractive optics and a focal plane array (front and side view, left) and an essentially two-dimensional form-factor for a distributed aperture imager with comparable aperture size and hence resolution capability (front and side view, right).

Because of the relatively long wavelengths of mmW radiation as compared to those in the optical spectrum, large aperture sizes are needed to achieve sufficient resolution for most applications of interest. For conventional imaging systems consisting of refractive optics and a focal plane array, increasing aperture size results in volumetric scaling of the imager with commensurate weight increase. In contrast, a distributed aperture imaging system is essentially two-dimensional in nature and can achieve effectively large apertures, thus providing the requisite resolution in a smaller form factor, as illustrated in Figure 1. In comparing the two approaches in this figure it should be pointed out that additional hardware is required for processing the collected signals; that is, only the front-end of the systems

is represented here. However, back-end hardware for the distributed aperture imager potentially can be made small and lightweight, thus maintaining its advantage over the conventional imager approach [7].

2. PHENOMENOLOGY MEASUREMENTS

To best represent the brownout conditions that U.S. military helicopters encounter abroad in theater, testing was undertaken at Yuma Proving Grounds in Yuma, AZ. Several airframes were tested to best represent the various brownout conditions that occur during landing in an unimproved landing zone. These tests were considered “worst case” as the conditions were such that the ground was as dry as possible, and the soil in a 240’ wide lane was tilled 8 inches deep to produce the largest dust cloud possible. The imaging system was set at one side of the lane and a reflector, tilted to reflect zenith ‘cold sky’, was set at the other with the imager focused at the reflector. A helicopter then flew over the lane to simulate brownout conditions while the imager stared at the reflector to measure signal loss through the dust.

Of the three platforms tested, the largest platform caused a 20% signal degradation in a “worst case” scenario possible. It was considered “worst case” because the imager was only a few meters off the ground and therefore was staring through the largest particles furthermore the imager was looking through both sides of the cloud surrounding the helicopter whereas the pilot only sees through half of the cloud. Figure 2 illustrates the layout of the test arrangement and a graph of the signal degradation. A more detailed description of the testing conditions may be found in a previous publication [6].

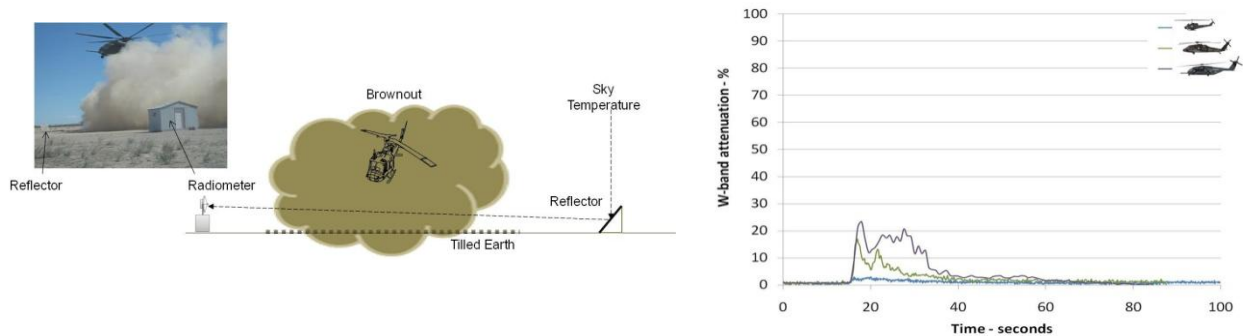


Figure 2: Dynamic W-band dust cloud attenuation setup at YPG used to measure the attenuation due to dust clouds for small, medium, and large, rotary aircraft (left) and plot of attenuation within the W-band during the rotary craft flyovers (right).

3. DEVELOPMENTS IN ENABLING TECHNOLOGIES

To fully realize a 220 channel W-Band imager, several enabling technologies had to be developed to meet our specifications of size, weight, and power (SWaP), resolution, field of view (FoV), and signal to noise ratio (SNR). While there are many components available for commercial purchase, few of them meet our size, weight, and power specifications to allow the intended imager to qualify as flight worthy. With the advent of these enabling technologies, we transitioned our system from a periodic regularly spaced array (Pathfinder I) to an aperiodic, non-regularly spaced array (Pathfinder II) to test these enabling technologies in a relevant system and validate the performance of the new hardware.

3.1 Control Electronics

The previous electronics layout for the power distribution, image processing, and phase control involved a rack mounted system of various FPGAs and a full desktop computer. Altogether this system weighed over 100 pounds and occupied around 2 cubic meters of space. For the purposes of demonstrating that the technology worked, this setup was acceptable in a lab environment. To make the system portable and eventually flyable, great reductions in size, weight, and power were necessary. To accomplish these tasks, PSI partnered with EM Photonics (EMP) to

develop proprietary electronics that would greatly reduce size, weight, and power to manageable levels and thus allow the system to fit the form factor for an imager to be attached to a helicopter.

One of the first steps was to reduce the FPGA system down to the board level. To accomplish this, EMP designed a custom FPGA board and a custom distribution board capable of handling 32 channels, thereby reducing the circuit board count of the power distribution to two boards. In this upgrade, the receiver board for the phase control was also redesigned with a 220 channel system in mind. Our previous receiver board was a discrete detector board, where there was one detector for each channel in the system. For a 30 channel system this was feasible as there was enough room for relatively large detectors on a circuit board. Because of the spacing issues the optics included 15x magnification to scale the fiber array output to the detectors. But to scale to 220 channels, a more compact solution was needed as the board would grow massive quickly. To reach the goals set forth, an InGaAs Focal Plane Array was utilized. This allowed us to take out the magnification previously needed in the optical pathway. It also reduced the total area of the detector array to the size of a common CPU, saving space and weight. Figure 3 shows the old rack mounted electronics, while Figure 4 displays the new hardware custom built to reduce size, weight, and power.

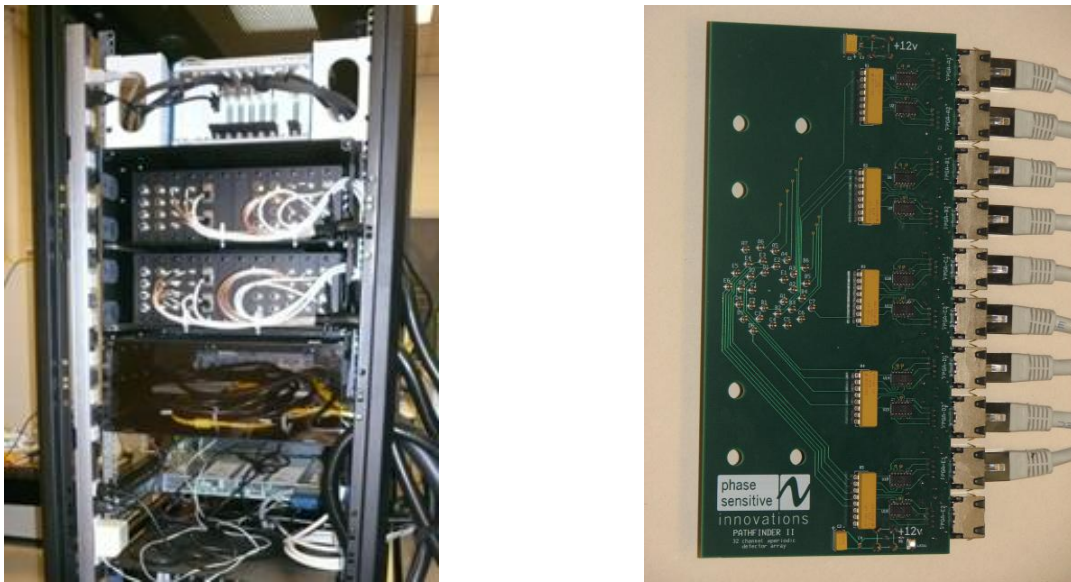


Figure 3: Rack mounted FPGA and distribution system (left) and Discrete Detector Receiver Board (right).

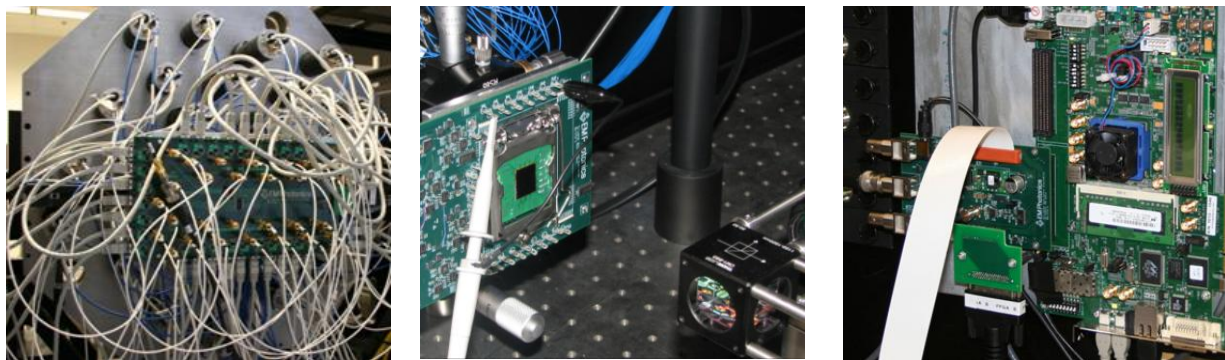


Figure 4: New Distribution Board attached to antenna array (left), FPA Receiver Board (middle), and FPGA Board (right).

Future work in this area will comprise finishing design and delivery of power and signal distribution boards for the full 220 channel system and developing a power supply and regulation scheme to allow the imager to work when attached to a helicopter.

3.2 Optics

To accommodate the new antenna array layout, the requisite optical fiber array and microlens array were also needed. As we needed custom designed, aperiodic optical fiber and microlens arrays, we were driven to create our own in house.

The Fiber Array consists of an optical fiber bundle held in place by being glued into a patterned silicon face plate that rests in an aluminum housing. The face plate is manufactured by through wafer etching holes in the pattern from the antenna array into a piece of silicon. The silicon is then cut to size and inserted into the aluminum housing. The aluminum housing serves to hold the face plate and to mate to the optical processor in the imager. After the fibers are individually glued into place in the Si face plate and UV cured, the fibers are set in place with a viscous epoxy to give the bundle strength rigidity. The microlens array is patterned to be an exact match of the Si face plate. A fused silica wafer is spun in resist and the pattern is applied via lithographical processes. The array is then cut to size and placed in the optical network after the fiber array to collimate the beams of each fiber individually. Figure 5 shows the optical fiber and microlens arrays. A more detailed discussion of the optical components was published previously[9].

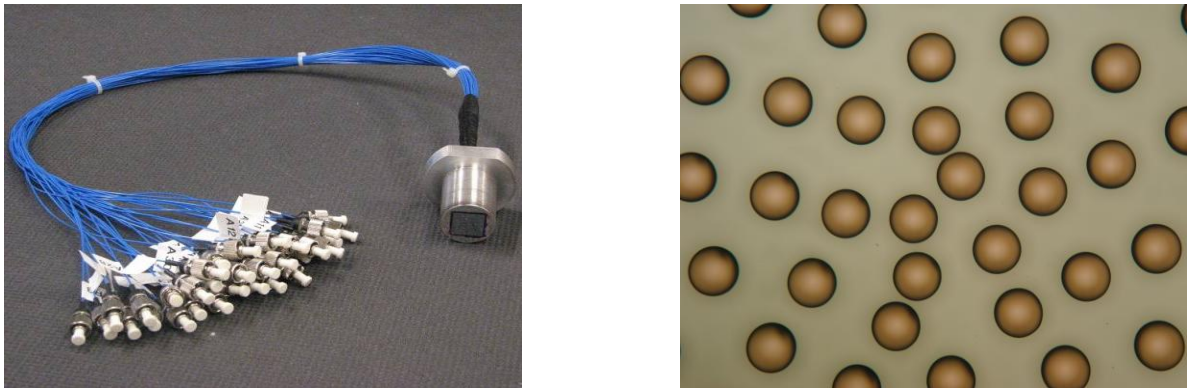


Figure 5: Aperiodic Optical Fiber array (left) and Aperiodic microlens array (right).

4. 30 ELEMENT APERIODIC ARRAY IMAGERY

To increase the alias free field of view of Pathfinder I, a new antenna array was fabricated to hold the antenna modules in an aperiodic, non-regular spaced layout. When this was in place, the new electronics and optics were added to test their functionality prior to placing them in the final 220 channel W-Band imager. Figure 6 shows pictures of Pathfinder I and Pathfinder II while Figure 7 shows the requisite antenna layouts with measured and simulated Point Spread Functions.



Figure 6: Pathfinder I antenna array (left) and Pathfinder II antenna array (right).

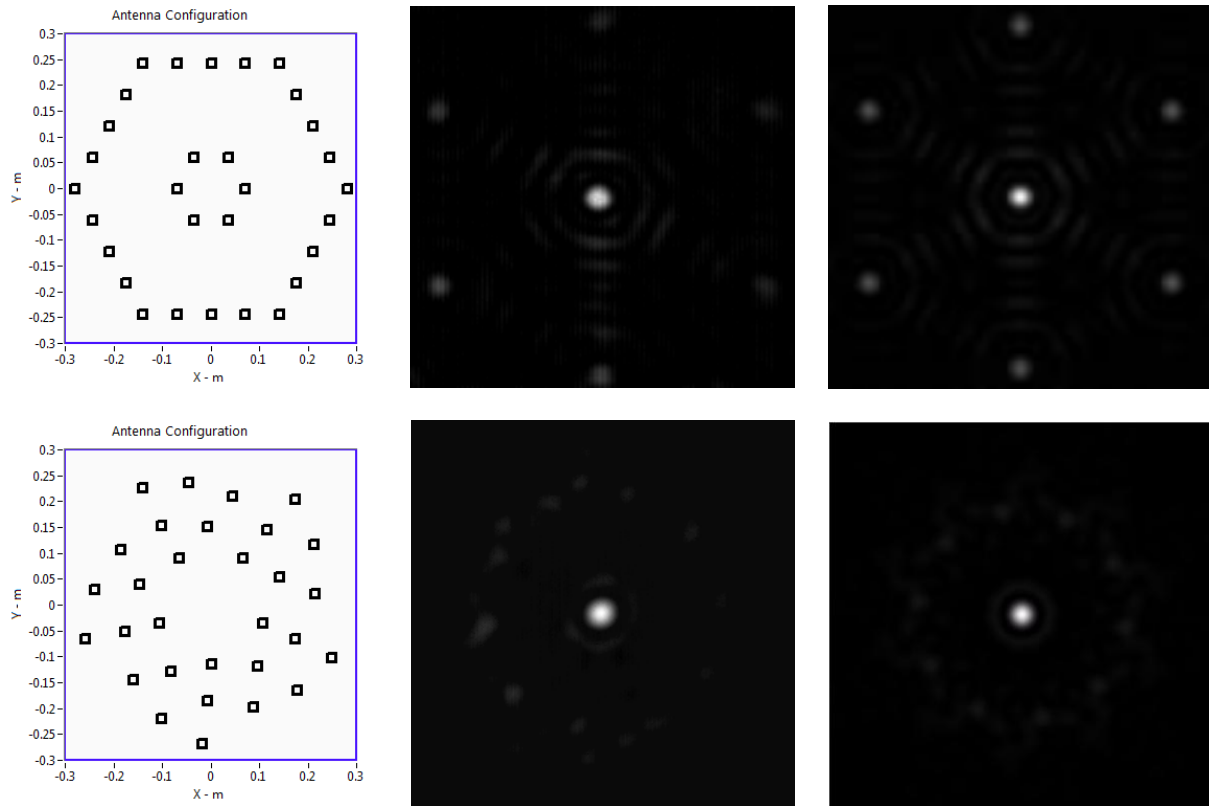


Figure 7: Antenna array configuration (left), measured point spread function (middle), and simulated point spread function (right). The upper row corresponds to the Pathfinder I, while the lower row corresponds to Pathfinder II.

It is apparent from examining Figure 7 that the hexapolar aliasing present in the PSF from the Pathfinder I system is no longer present in the Pathfinder II system. There are, however, the existence of prominent side lobes, especially two rings that surround the main beam. This is a consequence of the low channel count of the imager, which remains at 30 channels due to the limited number of available LNAs. These side lobes contribute to noise in the periphery of the images that can be seen in the compilation of passive imagery presented in Figure 8. Moving to higher channel count will further mitigate side lobe levels, enhancing future imagery.

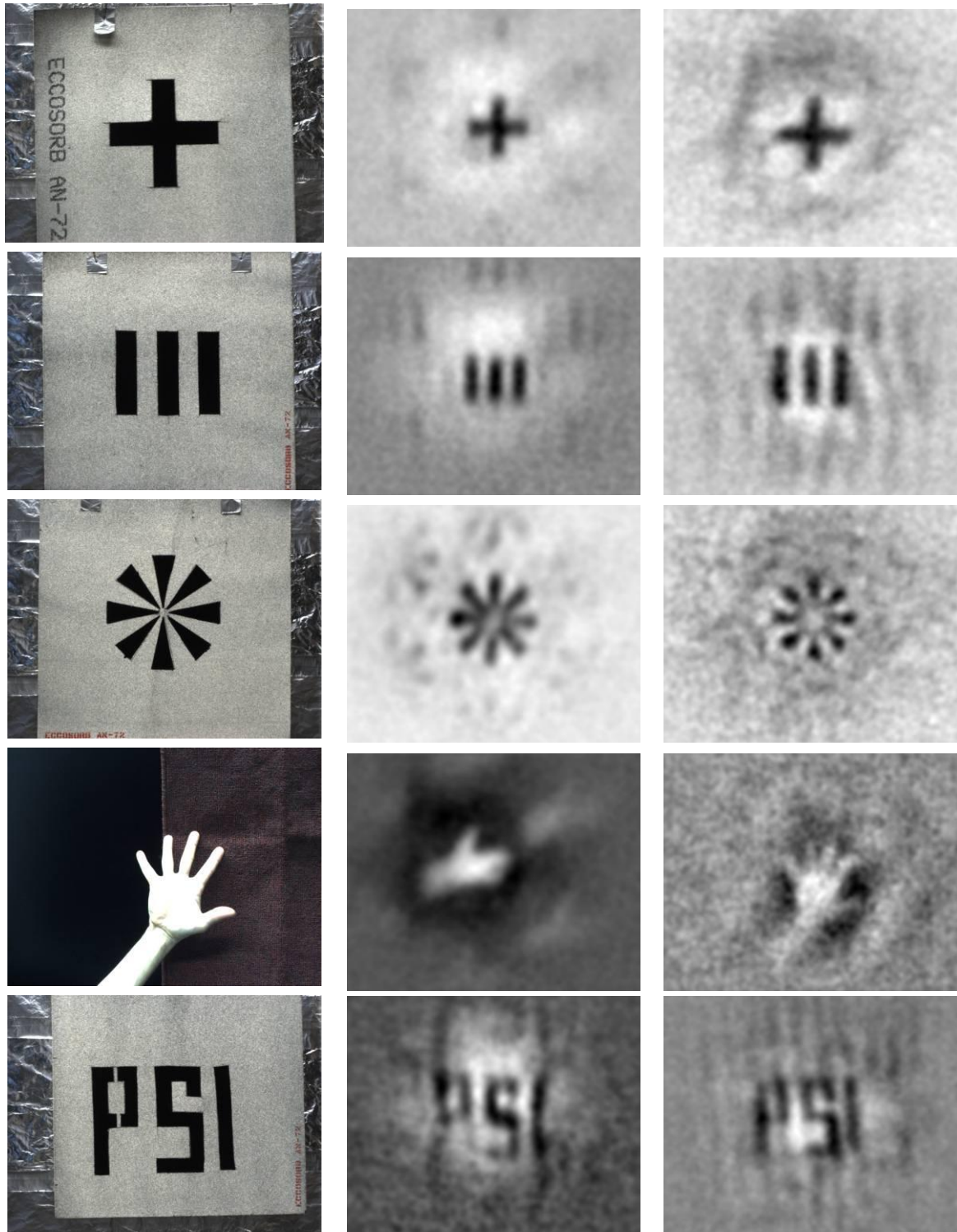


Figure 8: Comparison of passive imagery collected by the Pathfinder I (middle) and Pathfinder II (right) imagers for various scenes (left).

5. CONCLUSIONS AND FUTURE WORK

We have presented our updated passive millimeter wave imaging system utilizing an aperiodic distributed aperture antenna array and optical upconversion. Phenomenology studies of the brownout conditions that we plan on operating in have been reviewed and presented. Also discussed were advancements in enabling technologies that have helped us progress towards our final goal of a 220 channel W-band imager to assist in brownout mitigation. Finally, imagery from the upgraded system was demonstrated and compared to previous imagery from the former periodic incarnation of the system to show progress in suppressing side lobes in the imagery. This imagery was collected at video frame rates.

Future work on this project will entail utilizing the components and techniques developed in the change from Pathfinder I to II to further miniaturize the system to become flight worthy. As new enabling technologies become available they will need to be rigorously tested to validate performance so that there is the necessary confidence level afforded to warrant a flight test on an actual helicopter platform.

6. ACKNOWLEDGMENTS

We would like to thank Dr. Elizabeth Twarog, Dr. Dave Dowgiallo, and Dr. Peter Gaiser of the Naval Research Laboratory and their colleagues as well as Dr. Michael Duncan at the Office of Naval Research – Information, Electronics, and Surveillance Division for providing technical oversight regarding various aspects of this work.

7. REFERENCES

- [1] F. T. Ulaby, R. K. Moore, and A. K. Fung, Microwave Remote Sensing: Active and Passive, Vol. I – Microwave Remote Sensing Fundamentals and Radiometry, Addison-Wesley, Reading, Massachusetts, 1981.
- [2] D. M. Sheen, D. L. McMakin, and T. E. Hall, "Three-Dimensional Millimeter-Wave Imaging for Concealed Weapon Detection," *IEEE Transactions on Microwave Theory and Techniques*, Volume 49, pp. 1581-1592, 2001.
- [3] L. Yujiri, M. Shoucri, and P. Moffa, "Passive Millimeter-Wave Imaging," *IEEE Microwave Magazine*, pp. 39-50, September 2003.
- [4] Major D. W. Pendall, "Persistent Surveillance and Its Implication for the Common Operating Picture," *Military Review*, pp. 41-50, November-December 2005.
- [5] S. Scheduling, G. Brooker, R. Hennessy, M. Bishop, and A. Maclean, "Terrain Imaging and Perception using Millimetre Wave Radar," *Proc. 2002 Australasian Conference on Robotics and Automation*, pp. 60-65, 2002.
- [6] C. A. Schuetz, E. L. Stein, Jr., J. Samluk, D. Mackrides, J. P. Wilson, R. D. Martin, T. E. Dillon, and D. W. Prather, "Studies of Millimeter Wave Phenomenology for Helicopter Brownout Mitigation," *Proceedings of SPIE*, Volume 7485, 2009.
- [7] Thomas E. Dillon, Christopher A. Schuetz, Richard D. Martin, Shuoyuan Shi, Daniel G. Mackrides, and Dennis W. Prather, "Passive Millimeter Wave Imaging Using a Distributed Aperture and Optical Upconversion," *Proceedings of SPIE*, Volume 7309, 2010.
- [8] C. A. Schuetz, J. Murakowski, G. J. Schneider, and D. W. Prather, "Radiometric millimeter-wave detection via optical upconversion and carrier suppression," *IEEE Transactions on Microwave Theory and Techniques*, Volume 53, pp. 1732-1738, 2005.
- [9] T. E. Dillon, C. A. Schuetz, R. D. Martin, E. L. Stein, Jr., J. P. Samluk, D. G. Mackrides, M. S. Mirotznik, and D. W. Prather, "Optical Configuration of an Upconverted Millimeter-Wave Distributed Aperture Imaging System," *Proceedings of SPIE*, Volume 7485, 2009.